Burial and exhumation history of the Jameson Land Basin, East Greenland, estimated from thermochronological data from the Blokelv-1 core

Paul F. Green and Peter Japsen

Apatite fission-track analysis (AFTA) data in two Upper Jurassic core samples from the 231 m deep Blokelv-1 borehole, Jameson Land, East Greenland, combined with vitrinite reflectance data and regional AFTA data, define three palaeo-thermal episodes. We interpret localised early Eocene (55–50 Ma) palaeotemperatures as representing localised early Eocene heating related to intrusive activity whereas we interpret late Eocene (40–35 Ma) and late Miocene (*c*. 10 Ma) palaeotemperatures as representing deeper burial followed by successive episodes of exhumation. For a palaeogeothermal gradient of 30°C/km and likely palaeo-surface temperatures, the late Eocene palaeotemperatures require that the Upper Jurassic marine section in the borehole was buried below a 2750 m thick cover of Upper Jurassic – Eocene rocks prior to the onset of late Eocene exhumation. As these sediments are now near outcrop at *c*. 200 m above sea level, they have been uplifted by at least 3 km since maximum burial during post-rift thermal subsidence. The results are consistent with estimates of rock uplift on Milne Land since the late Eocene and with interpretation of Ocean Drilling Program (ODP) data off South-East Greenland suggesting that mid-Cenozoic uplift of the margin triggered the marked influx of coarse clastic turbidites during the late Oligocene above a middle Eocene to upper Oligocene hiatus.

Keywords: East Greenland, Jameson Land, Upper Jurassic, apatite fission-track analysis, burial, exhumation

P.F.G., *Geotrack International, 37 Melville Road, Brunswick West, Victoria 3055, Australia*.
E-mail*: mail@geotrack.com.au*
P.J.*, Geological Survey of Denmark and Greenland, Øster Voldgade 10, DK-1350 Copenhagen K, Denmark*

With sedimentary basins offshore East Greenland yet to be drilled, the onshore Jameson Land Basin (Surlyk 2003) provides a window into the nature of potential Jurassic source-rock sequences in offshore basins. Understanding the thermal history and maturity development in the onshore sequences can therefore provide unique insights into the prospectivity of the offshore basins. The Jameson Land Basin has itself been the focus of hydrocarbon exploration by a group of concessionaries with Atlantic Richfield (ARCO) as operator, but in 1990 the group decided not to continue exploration (Christiansen *et al*. 1992; Mathiesen *et al*. 2000). One of the main geological risks that ARCO critically assessed was the thermal maturity of their main target, the Upper Permian carbonates, since earlier studies had concluded that Tertiary exhumation had removed up to 3 km of Cretaceous sediments and Paleocene–Eocene volcanic rocks across the basin (Christiansen *et al*. 1992). Currently, Greenland Gas and Oil A/S and Nunaoil A/S hold a hydrocarbon exploration and exploitation licence across much of the Jameson Land Basin (*www.govmin.gl*).

Presented here is a thermal history study of samples obtained from the core from the Blokelv-1 borehole, drilled by GEUS in 2008 to provide detailed information about the Upper Jurassic stratigraphy and petroleum system of the Jameson Land Basin (Fig. 1). GEUS suc-

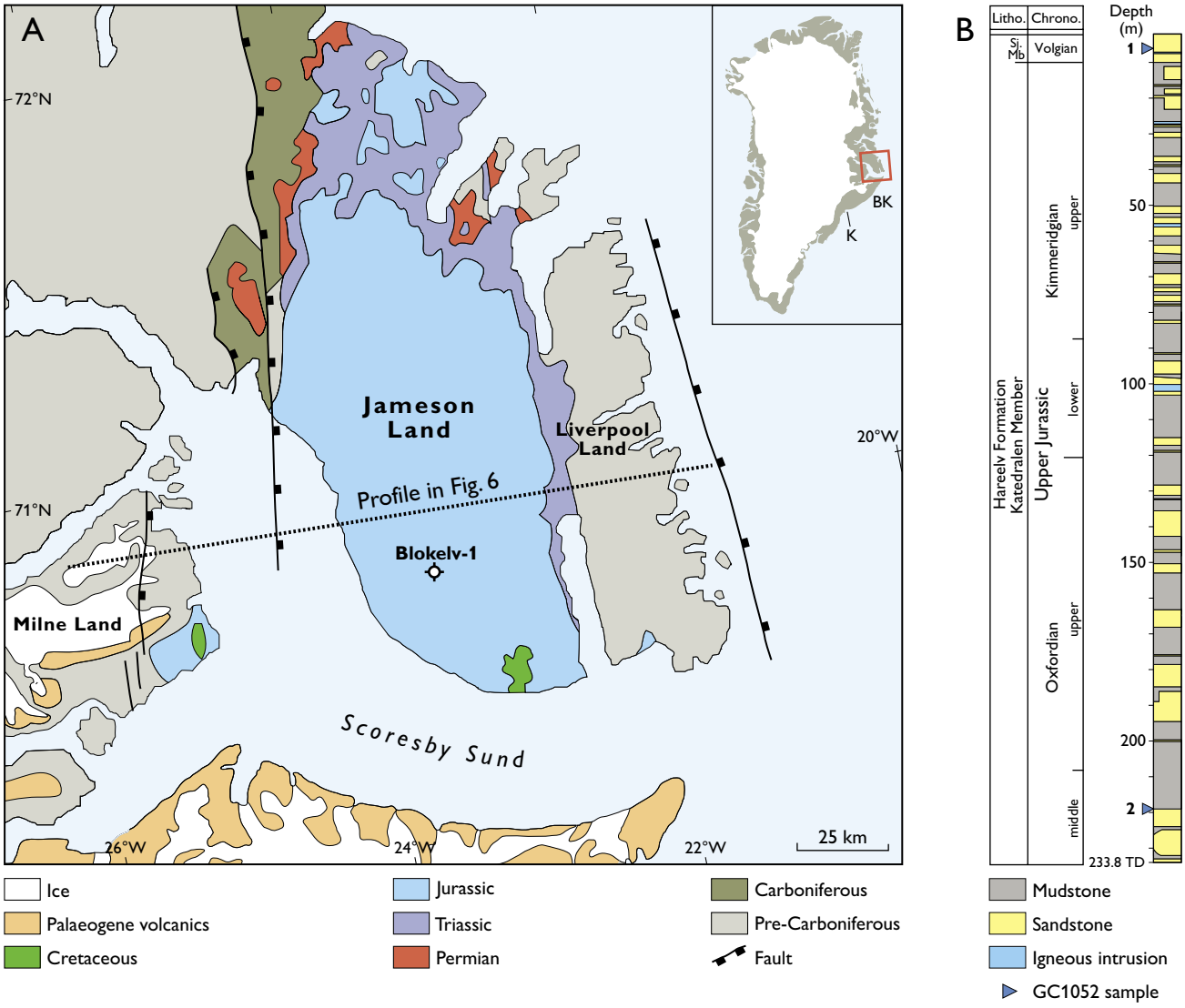

Fig. 1. **A**: Simplified geology of the Jameson Land Basin and adjacent areas showing the location of the Blokelv-1 borehole (modified after Surlyk 2003); inset shows the location of the study area in East Greenland. **BK**: Blosseville Kyst. **K**: Kangerlussuaq. **B:** Stratigraphic column of the Blokelv-1 borehole showing the stratigraphic level of the two samples used in this study (**1**, GC1052-1; **2**, GC1052-2). Log modified from Bjerager *et al.* 2018a, this volume). Litho: Lithostratigraphic subdivision. Chrono: Chronostratigraphic subdivision. **Sj. Mb**: Sjællandselv Member. **TD**: Total depth.

cessfully drilled and cored the Blokelv-1 borehole in the central part of the basin (ground level 200 m above sea level; a.s.l.), targeting the Upper Jurassic prolific source-rock interval of the Hareelv Formation (Bjerager *et al.* 2018a, this volume). The 231 m thick, marine succession cored in the Blokelv-1 borehole covers the middle Oxfordian to lower Volgian interval. The core has 100% recovery, and it consists of interlayered organic-rich, laminated mudstones, massive sandstones and heterolithic sandstone–mudstone intervals of the Katedralen Member and massive sandstones of the Sjællandselv Member of the Hareelv Formation. The recovered core is of very high quality and has been subject to an extensive sampling and analytical programme designed to investigate aspects of the petroleum geology of the Jameson Land Basin and published in nine papers (Ineson & Bojesen-Koefoed (eds) 2018, this volume). The dataset provides an excellent reference for Kimmeridge Clay Formation-equivalent deposits in the North Atlantic area.

At first glance, the relatively low-lying landscape of the Jameson Land Basin is in sharp contrast to the high terrains of the volcanic province along Blosseville Kyst to the south of Scoresby Sund, where elevations reach 3.7 km a.s.l. This might initially suggest that Jameson

Land has undergone a less complex post-Jurassic history of uplift and erosion compared to regions to the south. However, thermochronological data from the Jurassic sediments of the Jameson Land Basin presented here (see also Mathiesen *et al*. 2000; Hansen *et al*. 2001) provide evidence of post-Jurassic burial and exhumation that is surprisingly similar to the region around Kangerlussuaq, to the south (Larsen & Saunders 1998; Brooks 2011; Bonow *et al*. 2014; Japsen *et al*. 2014).

Thermal history interpretation

AFTA data

Two sandstone core samples from the lower and upper levels of the Blokelv-1 borehole (Fig. 1B) were processed for apatite fission-track analysis (AFTA), and both samples gave excellent apatite yields. Apatite fission track ages of 50.4 ± 6.2 Ma and 38.5 ± 4.0 Ma in the two samples are much less than the depositional age of the sampled units; at depths of less than 250 m (and present-day temperatures less than 20°C), this degree of age reduction immediately shows that the sampled units have been much hotter in the past. Mean track lengths of 12.25 ± 0.22 μm and 11.71 ± 0.23 μm also demonstrate that these samples have been hotter in the past, prior to cooling to present-day temperatures.

Full details of the AFTA data are provided in Appendix 1. Quantitative thermal history constraints have been extracted from the data using principles outlined by Green & Duddy (2012) and Green *et al*. (2013), with results summarised in Table 1. AFTA data from both samples provided highly reliable thermal history constraints.

Thermal history interpretation of AFTA data

The AFTA data in sample GC1052-1 can be explained in terms of two palaeo-thermal episodes, as detailed in Table 1. In contrast, the AFTA data in sample GC1052-2 require three palaeo-thermal episodes to explain all aspects of the data, although the precise timing of the earliest episode cannot be defined with confidence. This is because the palaeotemperature of 100–110°C in the second episode produced almost total annealing of all tracks formed up to that time, largely masking the previous history. On the basis of evidence discussed below, we

Table 1. Palaeotemperature analysis summary: AFTA and VR data from the Blokelv-1 borehole

Sample number GC1052-	Mean depth (m below KB)	Present temperature* (°C)	Stratigraphic age (Ma)	VR** (%)	Maximum palaeotemp.+ (°C)	Onset of cooling+ (Ma)	Maximum palaeotemp.+ (°C)	Onset of cooling+ (Ma)
1	**6**	**5**	**159–146**		**100–105**	**58–28**	**70–80**	**17–5**
	23.59		159–146	0.52	86			
	32.78		159–146	0.54	90			
	68.77		159–146	0.50	83			
	80.77		159–146	0.55	91			
	92.74		159–146	0.56	93			
	104.79		159–146	-	-			
	116.82		159–146	0.56	96			
	152.75		159–146	0.61	100			
	164.82		159–146	0.68	113			
	176.77		159–146	0.62	102			
	188.77		159–146	0.65	108			
	200.76		159–146	0.66	109			
	212.77		159–146	0.78	125			
2	**219**	**12**	**159–146**		**>110**	**55–50?**		
					100–110	**50–28**	**80–85**	**13–3**
	224.74		159–146	0.74	121			
					Combined timing (Ma):	***55–50***		**13–5**
						50–28		

* Present temperature estimates based on an assumed surface temperature of 4°C, and an assumed thermal gradient of 30°C/km.

** From Bojesen-Koefoed *et al.* (2018).

+ Thermal history interpretation of AFTA data is based on an assumed heating rate of 1°C/Myr and a cooling rate of 10°C/Myr. Quoted ranges for palaeotemperature and onset of cooling correspond to ±95% confidence limits. Conditions shown in italics represent events that cannot be rigorously defined from the AFTA data.

Table 2. Intervals defining the beginning of episodes of cooling from AFTA data

	Onset of cooling (Ma)		
AFTA data	55–50	50–28	13–5
Blokelv samples			
GC1052-1, -2			
AFTA data (Study A)		40–30	10–5
AFTA data (Study B)	*	40–35	~10
Age of intrusion (Study C)	~53**		
	(55–51)		
Preferred regional timing	55–50	40–35	~10
	(early Eocene)	(late Eocene)	(late Miocene)
Dominant mechanism of cooling	Cooling after intrusive heating	Exhumation	Exhumation

Study A. 11 outcrop samples from northern East Greenland, north of the Jameson Land Basin, 72–74°N (Thomson *et al.* 1999).

Study B. 90 samples from outcrops and drillholes in a regional study of southern East Greenland focussed between 68 and 70°N (Japsen *et al.* 2014).

Study C. Analysis of the igneous intrusions in the Blokelv cored borehole (Larsen 2018, this volume).

*Japsen *et al.* (2014) related an event of cooling with overlapping timing (55–50 Ma) in southern East Greenland to the emplacement of the Kangerlussuaq Intrusion.

**The Blokelv sills are tholeiitic basalts considered to belong to the main group of dykes and sills in the Jameson Land Basin which has been dated at ~53 Ma. The intrusions form part of a 55–51 Ma group of tholeiitic basalt intrusions that were emplaced within the sedimentary basins in East Greenland (Larsen 2018, this volume).

infer that the earlier event in which this sample cooled below 110°C was related to igneous activity in the region (Larsen 2018, this volume), in the interval 55 to 50 Ma.

Timing constraints derived from AFTA data in each sample are listed in Table 1, and in Table 2 these constraints are compared with the timing of three Cenozoic cooling episodes defined from AFTA data in two previous studies of the East Greenland margin: (A) a study of the region north of the Jameson Land Basin (Thomson *et al*. 1999) and (B) a study in the Kangerlussuaq region to the south of Jameson Land (Japsen *et al*. 2014). The similarity in timing of the late Eocene and the late Miocene cooling episodes defined in this study and in the previous studies suggests that each represents a regional, synchronous cooling episode across the entire region, and by combining all constraints we arrive at our preferred timing of the onset of cooling in these events, between 40 and 35 Ma and ~10 Ma (Table 2). In addition to the episodes shown in Fig. 2, Japsen *et al*. (2014) also defined late Oligocene and early Miocene palaeo-thermal episodes in the region around Kangerlussuaq, but these are restricted to that region and do not extend to the Jameson Land Basin, so are not considered here.

We interpret the three events illustrated in Fig. 2 (from Table 2) in the following way:

55–50 Ma event. The timing of the early Eocene (55–50 Ma) event overlaps with that of intensive Palaeogene intrusive activity and correlates with the age of *c*. 53 Ma for dykes and sills in the Jameson Land Basin (Hald & Tegner 2000; Larsen 2018, this volume). Palaeotemperatures associated with this event are 100°C or above and are identified sporadically around the region (Japsen *et al*. 2014). On this basis, the palaeotemperatures characterising this episode are interpreted to be due either to contact or hydrothermal effects associated with igneous activity. No convincing evidence for any regional Paleocene to mid-Eocene cooling (related to exhumation) has been identified for samples in the area around Jameson Land (Thomson *et al*. 1999; Japsen *et al*. 2014), and the geological history recorded south of Jameson Land indicates that subsidence and burial dominated at the Palaeocene–Eocene transition (Brooks 2011; Bonow *et al*. 2014).

40–35 Ma event. Late Eocene cooling beginning between 40 and 35 Ma was interpreted largely in terms of regional uplift resulting in kilometre-scale exhumation by both Japsen *et al*. (2014) in the Kangerlussuaq region and Thomson *et al*. (1999) in the region to the north of Jameson Land. Japsen *et al*. (2014) interpreted the end-result of this phase of exhumation to have been a regional peneplain, the Upper Planation Surface (UPS) of Bonow *et al*. (2014). The presence of late Eocene intrusive bodies around Traill Ø (Price *et al*. 1997) suggests the possibility locally of a significantly elevated basal heat flow in this region at this time.

10 Ma event. Late Miocene cooling beginning at *c*. 10 Ma was again detected by both Japsen *et al*. (2014) in

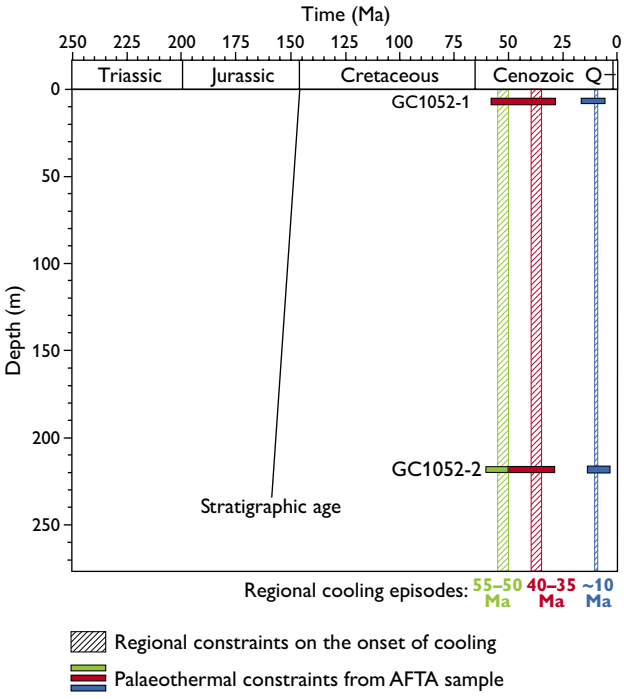

Fig. 2. Timing constraints on cooling episodes derived from AFTA data in two samples from the Blokelv-1 borehole (horizontal bars) plotted against depth. The regional constraints on the onset of cooling in three palaeo-thermal episodes (vertical bars) are based on AFTA data in the Blokelv samples and in regional studies (Table 2). **Q**: Quaternary.

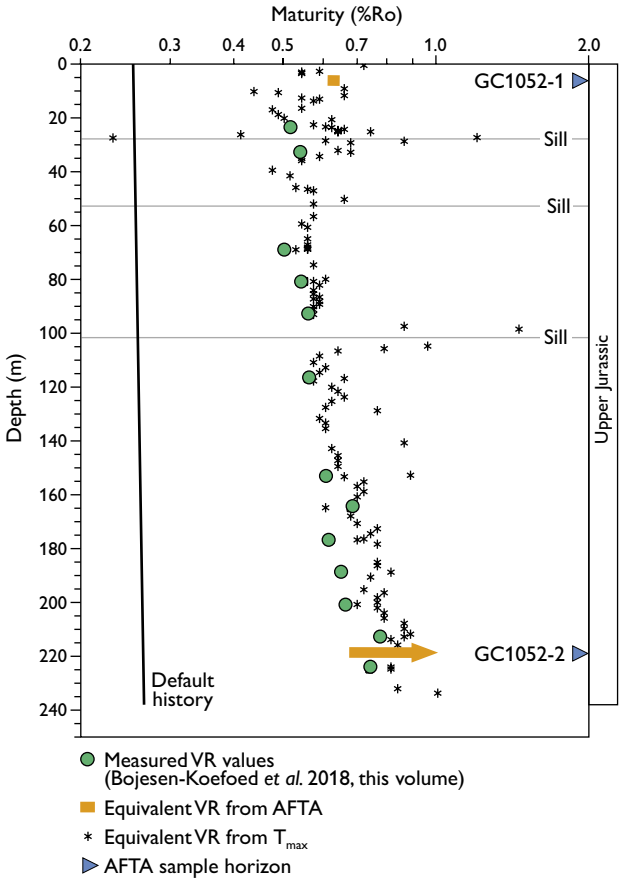

Fig. 3. Maturity indicators in samples from the Blokelv-1 borehole plotted against depth; VR values (Table 1) together with equivalent VR values (VReq) derived from Rock-Eval T_{max} data and equivalent ranges of VR defined from the AFTA data. Note that the orange arrow for the deeper sample indicates that the constraints on maturity from the AFTA data only provide a lower limit. The solid sub-vertical line shows the profile predicted from the "Default Thermal History", i.e., the history calculated from the assumption that all units throughout the well are currently at their maximum temperatures since deposition. The horizontal lines indicate the position of thin basaltic sills intruded into the Hareelv Formation (note the maturity effects close to these intrusions).

the Kangerlussuaq region and Thomson *et al.* (1999) to the north of Jameson Land. In both cases cooling was interpreted in terms of regional uplift resulting in kilometre-scale exhumation. Outcrop samples at low elevations around Kangerlussuaq cooled from peak palaeotemperatures around 60–70°C at this time. Japsen *et al.* (2014) interpreted these values to represent burial below the UPS that defines the present-day surface of elevated summits along the Blosseville Kyst.

Table 2 illustrates a high degree of consistency between the timing of cooling identified in this study and the dominant regional episodes identified by Thomson *et al.* (1999) and Japsen *et al.* (2014). On this basis, the results from sample GC1052-1 are interpreted as representing the two most recent episodes (i.e. late Eocene and late Miocene), while these two episodes as well as the early Eocene episode are recognised in sample GC1052-2.

Thermal history interpretation of vitrinite reflectance data

Results of vitrinite reflectance (VR) analyses are plotted against depth below surface in Fig. 3, together with equivalent VR (VR_{eq}) values derived from Rock-Eval T_{max} values (Bojesen-Koefoed *et al.* 2018, this volume). Also shown are the ranges of equivalent VR values (VR_{eq}) derived from AFTA data in samples GC1052-1 and -2 (defined by the maximum paleotemperature in each sample), together with the VR profile predicted on the basis

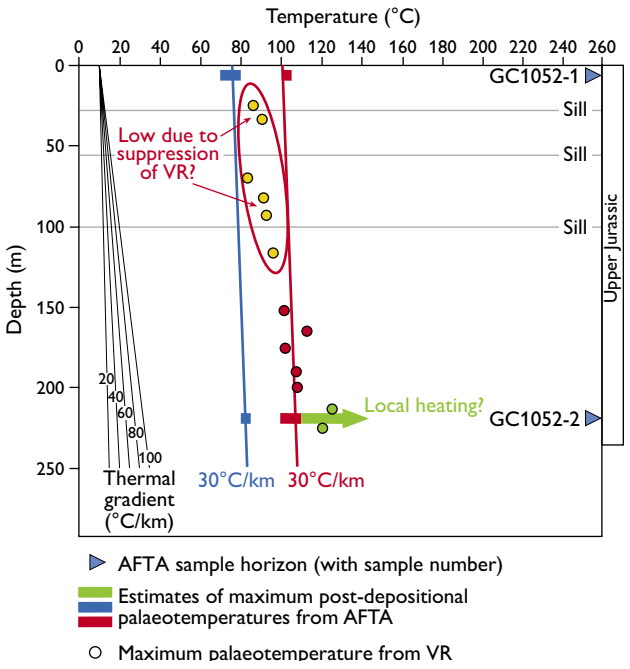

Fig. 4. Interpreted palaeotemperature profiles describing the palaeotemperatures in two episodes derived from AFTA and VR data in the Blokelv-1 borehole. Based on evidence from regional studies of East Greenland (Table 2), we interpret the early Eocene (55–50 Ma) maximum palaeotemperature (green arrow) revealed by AFTA data in sample GC1052-2 to represent localised heating due to intrusive activity. The late Eocene (40–35 Ma) and late Miocene (*c.* 10 Ma) palaeotemperatures (red and blue horizontal bars, respectively) revealed by AFTA are interpreted to represent the effects of burial, with late Eocene cooling representing the onset of regional, post-Jurassic exhumation, and late Miocene cooling representing the final phase of exhumation. It is thus inferred that the VR values recorded above 120 m in the borehole (yellow datapoints) are anomalously low due to suppression of reflectance in the source-rock facies (organic-rich mudstones) (Wilkins *et al*. 1992; Newman 1997). We regard the VR values below 120 m (red datapoints) as reliable indications of the degree of post-depositional heating. Linear profiles (red and blue lines) represent our preferred interpretation (based on regional data) involving palaeogeothermal gradients of ~30°C for the late Eocene and Miocene episodes.

of the Default Thermal History (i.e. the history expected if the section has never been any hotter than it is today). Both VR and VR_{eq} data plot well above the profile predicted by the Default Thermal History, confirming the evidence from AFTA that the sampled units have been hotter than their present-day temperatures at some time since deposition. Mean VR values tend to be slightly lower than the VR_{eq} values derived from the T_{max} data throughout the section. In general, T_{max} values tend to be sensitive to a range of factors and are not used quantitatively to provide estimates of maximum palaeotemperature in the way that VR data are. Note that the T_{max} data define local contact effects due to the three recognised intrusions, which the VR values do not show.

Maximum palaeotemperatures derived from the VR values (based on Burnham & Sweeney 1989) are listed in Table 2, and show a progressive downhole increase from 86°C to 125°C through the section intersected in the borehole. This apparent increase of *c.* 40°C over a depth interval of *c.* 200 m is equivalent to a thermal gradient of 200°C/km, which is well outside the range of typical sedimentary basin thermal gradients (Allen & Allen 2013). Integration of results from AFTA with the VR data resolves this apparent anomaly, as explained below.

Integration of AFTA and VR data, palaeotemperature profiles and mechanisms of heating and cooling

Palaeotemperature constraints from AFTA and the measured VR values are plotted against depth in Fig. 4. Maximum palaeotemperatures derived from VR values at depths between 20 m and 120 m are *c.* 10–20°C lower than the late Eocene palaeotemperature range of 100–105°C indicated by AFTA data in sample GC1052-1 at similar depths. In contrast, maximum palaeotemperatures of *c.* 125°C derived from the two deepest VR values at depths of 210–225 m are higher than the late Eocene palaeotemperatures derived from AFTA in sample GC1052-2 at a similar depth. They are, however, consistent with the early Eocene palaeotemperature defined from AFTA data in this sample. Furthermore, as illustrated in Fig. 4, maximum palaeotemperatures derived from VR values between 150 m and 200 m are consistent with the trend of the late Eocene palaeotemperatures derived from AFTA in samples GC1052-1 and -2.

We interpret the mismatch at shallow depths between VR values and the late Eocene palaeotemperature range from AFTA in sample GC1052-1 as due to suppression of reflectance levels at these depths. Suppression is commonly observed in Upper Jurassic organic-rich mudstones of the North Atlantic region (Wilkins *et al.* 1992; Newman 1997). Bjerager *et al.* (2018b, this volume) and Bojesen-Koefoed *et al.* (2018, this volume) provided detailed discussions of the differences between the organic material above and below *c.* 100 m in the cored interval. They showed that at shallow depths, amorphous marine

organic material dominate whereas an increased content of terrigenous organic material occurs at depth.

As illustrated in Fig. 4, maximum palaeotemperatures from VR data at depths between *c*. 150 m and 200 m, together with late Eocene palaeotemperatures derived from AFTA in samples GC1052-1 and -2 define a linear profile characterised by a palaeogeothermal gradient around 30°C/km. Late Miocene palaeotemperatures defined from AFTA in the two samples are also consistent with a similar palaeogeothermal gradient. This gradient contrasts markedly with the apparent gradient of *c*. 200°C/km defined by the VR data (see above), and is more typical of heating related to deeper burial.

Accepting this interpretation, units throughout the borehole underwent a major phase of cooling in the late Eocene (beginning between 40 and 35 Ma), followed by a later phase of cooling in the late Miocene (*c*. 10 Ma). Most units cooled from maximum post-depositional palaeotemperatures in the late Eocene event but locally some horizons reached higher palaeotemperatures in the early Eocene, presumably reflecting the effects of intrusive bodies. This interpretation is consistent with the results reported from the Kangerlussuaq region to the south by Japsen *et al*. (2014), who regarded the late Miocene and late Eocene cooling episodes as representing successive episodes of exhumation, while early Eocene events were interpreted as local effects associated with igneous intrusions.

Thermal history synthesis

On the basis of the discussion presented above, we interpret the palaeotemperature constraints derived from AFTA and VR data in the Blokelv-1 borehole as representing the combined effects of deeper burial followed by successive episodes of exhumation in the late Eocene and Miocene, as well as localised early Eocene heating due either to contact heating or hydrothermal effects associated with intrusive activity. The results provided here are highly consistent with regional data and the interpretation presented here is regarded as reliable.

Thermal history reconstruction

Here we present reconstructed thermal and burial-uplift histories for the Upper Jurassic section intersected in the Blokelv-1 borehole (Fig. 5) based on the results presented above. It should be emphasised that while the preferred reconstruction illustrated here provides a satisfactory explanation of the AFTA and VR data from this well, the reconstruction is not unique. Therefore, it is important to appreciate those aspects of the histories that are constrained by the data, and those that are not.

Factors that can be confidently defined in this study (within the limits of analytical uncertainty) include: (a) magnitude of heating at the palaeothermal maximum and the subsequent palaeothermal peaks and (b) timing of the onset of cooling in each episode. Factors that can be defined when samples are available over a sufficiently large range of depths or elevations, but cannot be constrained in this study include: (a) palaeogeothermal gradients during each episode and (b) additional burial during each episode for a specified value of palaeogeothermal gradient. Aspects which cannot be uniquely defined in any situation include: (a) thermal history prior to the palaeo-thermal maximum and/or the subsequent palaeo-thermal peak, (b) amounts of re-burial between multiple episodes within a single unconformity and (c) detailed style of cooling history from each episode.

Figure 5A illustrates a possible thermal history reconstruction for the sedimentary units intersected in the Blokelv-1 borehole, based on the synthesis developed above. Key aspects of this reconstruction are:

- Surface temperature of 20°C at 30 Ma and earlier, decreasing to 10°C at 10 Ma and to a present-day value of 4°C over the last 12 Myr.
- Palaeogeothermal gradient of 30°C/km, constant to the present day.
- Localised heating within the vicinity of sample GC1052-2 to a palaeotemperature around 120°C, shown at *c*. 53 Ma but any time between 56 and 45 Ma is allowed by the regional timing constraints on this episode.
- An additional 2750 m of section deposited above the Upper Jurassic section intersected in the borehole, between 146 and 35 Ma (resulting in heating of sample GC1052-1 to *c*. 100°C prior to late Eocene cooling and exhumation).
- Subsequent removal of 1150 m (arbitrary) of section between 35 and 30 Ma, followed by deposition of a further 600 m (arbitrary) of section between 30 and 10 Ma.
- Removal of the remaining 2200 m of additional section between 10 Ma and the present day.

Note that the amount of re-burial between the two episodes of exhumation cannot be controlled by the data,

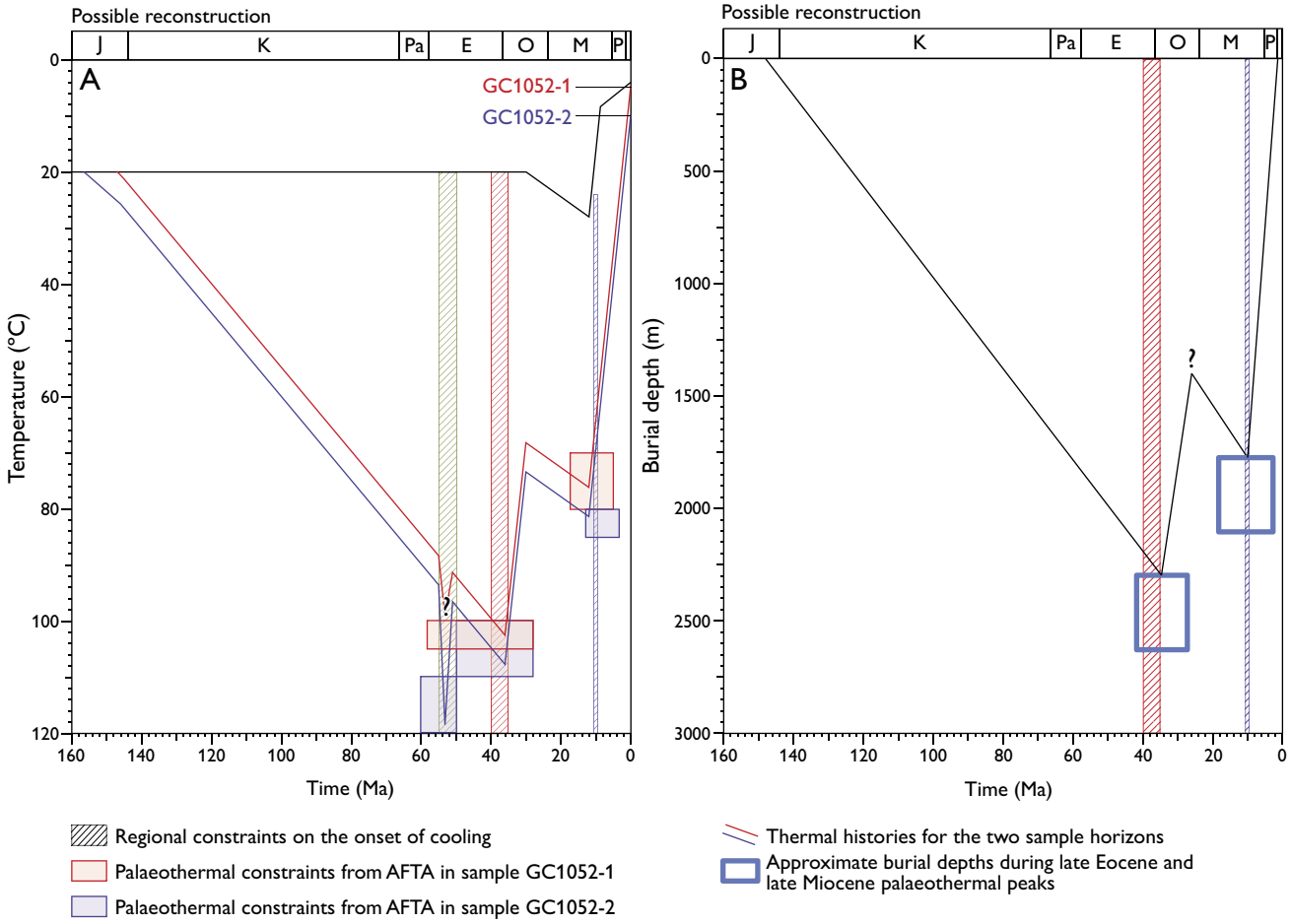

Fig. 5. Schematic illustration of the preferred thermal (A) and burial (B) history reconstruction for the section intersected in the Blokelv-1 borehole based on the AFTA and VR data. **J**: Jurassic. **K**: Cretaceous. **Pa**: Palaeocene. **E**: Eocene. **O**: Oligocene. **M**: Miocene. **P**: Pliocene. **A**: Comparison of palaeothermal constraints from AFTA in two samples (red and blue boxes) with thermal histories of the corresponding sample horizons (red and blue curves). The vertical columns show the preferred timing of three dominant palaeothermal episodes identified in the region (Fig. 2; Table 2). Black line at the top of the diagram defines the assumed palaeosurface temperature. **B:** Burial and exhumation history corresponding to A; the blue boxes show the approximate depth of burial during the late Eocene and late Miocene palaeothermal peaks. Note that no convincing evidence for regional Paleocene to mid-Eocene exhumation has been identified for samples in the area around Jameson Land (Thomson *et al.* 1999; Japsen *et al.* 2014).

and therefore also the amount of section removed in the initial episode beginning at 35 Ma is also not constrained. This reconstruction is considered to provide a reliable depiction of the post-depositional history of the Upper Jurassic section intersected in the Blokelv-1 borehole. Note that in this reconstruction, for the purposes of illustration, the localised heating around sample GC1052-2 at *c.* 53 Ma is shown as taking place over a duration of 2 Myr, as is the subsequent cooling. However, in reality heating and cooling would have been much more rapid, and for that reason the true maximum palaeotemperatures would have been much higher.

Comparison with previous studies

Magnitude of exhumation

Christiansen *et al.* (1992) presented the results of a first study of the exhumation of the Jameson Land Basin. They based their estimate on a range of observations including thermal maturity parameters, apatite fission-track parameters, porosity and seismic velocities; in particular they reported VR values up to 0.6% for organic-rich Permian and Jurassic formations at outcrop. They interpreted their data to indicate that between 1.5 and 3 km of overburden had been removed across the basin,

and that the lost cover likely consisted of more than 1 km of Cretaceous sediments as well as 1–2 km of Palaeogene basalts (primarily across the southern part of the basin).

Mathiesen *et al*. (2000) investigated the denudation history of the Jameson Land Basin using basin modelling constrained by apatite fission-track data. They concluded that the Upper Jurassic sediments that are exposed at the present day across Jameson Land were buried below a 2–3 km thick rock column: (1) a Cretaceous succession that varied from 1.3 km in the south to 0.3 km in the north; (2) a wedge of Palaeogene volcanics with a thickness of >2 km in the south thinning to <0.1 km in the north. According to their calculations, the erosion happened in response to tectonic uplift of *c*. 1 km. The magnitude of the section removed at the location of the Blokelv-1 borehole defined in this study (*c*. 2.8 km) thus agrees well with that estimated by Mathiesen *et al*. (2000) (removal of 2–3 km of section across Jameson Land).

Hansen *et al*. (2001) studied the late Mesozoic – Cenozoic thermal history of the Jameson Land Basin constrained by apatite and zircon fission-track data of Permian to Jurassic sedimentary rocks at outcrop. These authors interpreted their results in terms of regional thermal evolution related to burial leading to temperatures close to and in excess of the maximum temperatures of the apatite annealing interval (*c*. 125°C) followed by cooling mainly due to Cenozoic uplift and erosion. Furthermore, basaltic dyke and sill intrusions were found locally to cause resetting of apatite fission-track ages. These results are thus broadly in agreement with the conclusions presented here.

Our estimate of the magnitude of the section removed above the Blokelv-1 borehole (*c*. 2.8 km) agrees well with the results of Bonow *et al*. (2014) and Japsen *et al*. (2014) in their studies of the area between Milne Land and Kangerlussuaq (68–71°N) based on integration of evidence from stratigraphic landscape analysis, thermochronology and the stratigraphic record (Fig. 6). These authors argued that the present-day high elevation in East Greenland is the result of three tectonic phases of uplift and erosion during the Cenozoic that followed the eruption of voluminous flood basalts onto a largely horizontal lava plain near sea level at the Paleocene–Eocene transition (Larsen & Saunders 1998; Brooks 2011; Bonow *et al*. 2014), viz:

1. The late Eocene (*c*. 35 Ma) phase of uplift and erosion led to formation of an Oligo–Miocene erosion surface (peneplain) near sea level, the Upper Planation Surface (UPS).
2. Uplift of this surface in the late Miocene (*c*. 10 Ma) led to formation of a lower surface (the Lower Planation Surface, LPS) by incision below the uplifted UPS.
3. An early Pliocene uplift phase (*c*. 5 Ma) led to incision of valleys and fjords below the LPS, resulting in mountain peaks reaching 3.7 km a.s.l. Today, remnants of the UPS are preserved west of Jameson Land near the summits of Milne Land at *c*. 2 km a.s.l.

Bonow *et al*. (2014) estimated the magnitude of rock uplift at Milne Land to be *c*. 2.7 km based on Larsen *et al*.'s (1989) investigation of zeolite isograds (levels of equal thermal alteration; see also Neuhoff *et al*. 1997), and on their argument that the absence of the shallow and less altered zeolite zones may be explained by the removal of these zones by erosion. For Milne Land, they concluded that a section of about 900 m had been removed above the basalt flows that cover the summits there (assuming a palaeogeothermal gradient of 40°C at the time of zeolite formation). Bonow *et al*. (2014) then assumed that the palaeo-surface during the formation of the zeolites was near sea level (shortly after the eruption of the volcanics

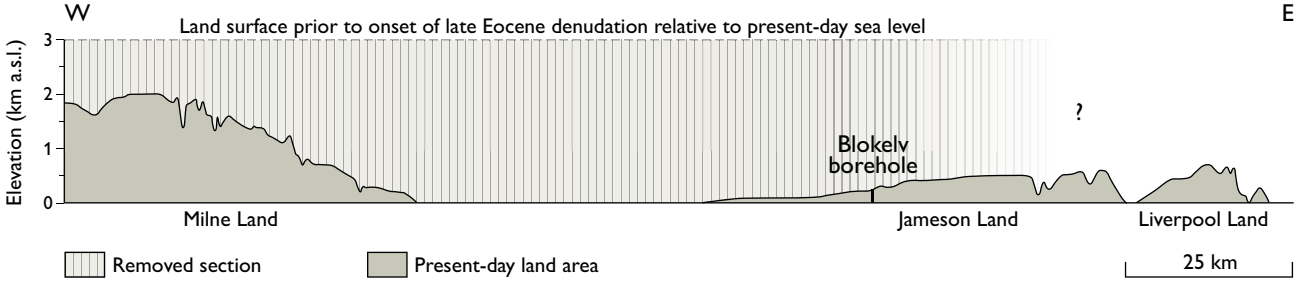

Fig. 6. Present-day elevation profile with indication of the section removed since late Eocene maximum burial. Based on Bonow *et al*. (2014) and Japsen *et al*. (2014). For location of profile, see Fig. 1.

at the Paleocene–Eocene transition at a time of regional subsidence; Brooks 2011). Consequently, the basalts, now at *c*. 1800 m a.s.l., have been uplifted 2700 m (i.e. 1800 + 900 m) since the formation of the zeolites in the Eocene.

Japsen *et al*. (2014) found that the UPS that defines the summits of Milne Land at *c*. 2 km a.s.l. represents the remnants of the Oligo-Miocene peneplain that was formed by erosion to sea level after late Eocene uplift and erosion, and that this peneplain was uplifted to its present elevation during uplift that began in the late Miocene. Assuming that the lost cover of 900 m (estimated from zeolite isograds) had been removed after late Eocene maximum burial, the magnitude of rock uplift was about 2.9 km since the late Eocene.

These estimates of the magnitude of rock uplift thus match those presented here because the Upper Jurassic marine sediments at outcrop (now at *c*. 200 m a.s.l.) at the Blokelv-1 location have been uplifted by a minimum of 3.0 km since their maximum burial below a (now lost) cover of *c*. 2.8 km in the late Eocene.

Timing of burial and exhumation

With no way of determining the timing of the onset of exhumation, Christiansen *et al*. (1992) and Mathiesen *et al*. (2000) assumed that the exhumation of the Jameson Land Basin accelerated after the Palaeogene volcanic eruptions. The present study, however, clearly shows that the onset of exhumation was in the late Eocene (*c*. 35 Ma) and documents that the exhumation process took place in at least two stages. These results thus imply that the section of rocks removed across Jameson Land not only included volcanic rocks extruded at the Paleocene–Eocene transition (as assumed by Mathiesen *et al*. 2000) but also a sedimentary cover deposited during the 20 Myr that followed the volcanic eruptions till the onset of exhumation in the late Eocene.

The geological record from the area south of Jameson Land confirms the timing of the Cenozoic events of burial and exhumation presented here. The area between Scoresby Sund and Kangerlussuaq subsided after continental breakup at 56 Ma. This is documented by the Igtertivâ Formation which immediately overlies the Main Basalts of Larsen *et al*. (1989, 2013) and includes volcanic flows interdigitated with marine sediments. The volcanic pile of the Main Basalts is up to 6 km thick and was erupted in less than 1 Myr (Pedersen *et al*. 1997). Subsidence continued during deposition of the fluvial to shallow-marine Kap Dalton Group (early to mid Lutetian), which interfingers with and overlies the Igtertivâ Formation in a downfaulted block at Kap Dalton (Larsen *et al*. 1989, 2005, 2013).

Results from ODP Site 918, off SE Greenland (Leg 152, *c*. 63°N) show that major uplift of the margin occurred long after continental break-up. Larsen *et al*. (1994) reported that the marine, lower Eocene sediments drilled there indicated low sedimentation rates with limited terrigenous influx before a middle Eocene to upper Oligocene hiatus. Larsen *et al*. (1994) thus argued that mid-Cenozoic uplift of the inner margin triggered the sudden, voluminous influx of coarse clastic turbidites at this ODP Site during the late Oligocene.

Uplift phases in the late Miocene and in the Pliocene are consistent with the late Miocene, early Pliocene and middle Pliocene ages of seismic sequence boundaries within the late Neogene and Quaternary deep-sea sedimentary succession off SE Greenland (Clausen 1998).

Conclusions

Three palaeo-thermal episodes affected the Upper Jurassic sediments penetrated by the Blokelv-1 borehole based on AFTA and VR data combined with regional AFTA data. These episodes are interpreted to be due to the following mechanisms:

- Early Eocene (55–50 Ma) palaeotemperatures represent localised early Eocene heating related to intrusive activity.
- Late Eocene (40–35 Ma) palaeotemperatures represent deeper burial followed by exhumation.
- Late Miocene (*c*. 10 Ma) palaeotemperatures represent deeper burial followed by exhumation.

The presence of two elevated planation surfaces in the region that were formed and uplifted after the volcanic eruptions supports the interpretation of the palaeothermal data in terms of episodic rather than monotonic cooling (Bonow *et al*. 2014; Japsen *et al*. 2014).

The late Eocene palaeotemperatures require that *c*. 2800 m of Upper Jurassic – Eocene rocks covered the Upper Jurassic section in the borehole prior to the onset of late Eocene exhumation, assuming a palaeogeothermal gradient of 30°C/km and likely palaeo-surface temperatures. This implies that maximum burial in the Jameson Land Basin was achieved long after the rift climax in central East Greenland at the Jurassic–Cretaceous tran-

sition (Surlyk 2003) and after the volcanic eruptions that accompanied break-up in the north-east Atlantic at the Paleocene–Eocene transition (Pedersen *et al*. 1997).

As the Upper Jurassic sediments at the location of the Blokelv-1 borehole now crop out at *c*. 200 m a.s.l., they have been uplifted by at least 3 km since maximum burial during post-rift thermal subsidence. Such a magnitude of rock uplift is comparable with estimates from Milne Land where a regional peneplain (the upper planation surface, UPS) defines the summits at *c*. 2 km a.s.l. This surface was formed by erosion to sea level (after removal of a rock column of *c*. 900 m) following late Eocene uplift and subsequently uplifted to its present elevation during uplift that began in the late Miocene. Consequently, the rock uplift on Milne Land was *c*. 2.9 km since the late Eocene. Rock uplift in the order of 3 km since the late Eocene has thus affected a wide area, far beyond the boundaries of the Jameson Land Basin.

That strong uplift of the East Greenland margin began at the Eocene–Oligocene transition is supported by interpretation of ODP data off South-East Greenland which suggest that uplift of the margin at this time triggered the marked influx of coarse clastic turbidites during the late Oligocene above a middle Eocene to upper Oligocene hiatus.

Acknowledgements

We acknowledge the pertinent and constructive comments of the referees, Andrew Carter and Andrew G. Whitham. Jette Halskov and Stefan Sølberg are thanked for graphical support.

Reference list

Allen, P.A. & Allen, J.R. 2013: Basin analysis: Principles and application to petroleum play assessment, 632 pp. Indianapolis: John Wiley & Sons.

Bjerager, M., Bojesen-Koefoed, J. & Piasecki, S. 2018a: The Upper Jurassic Blokelv-1 cored borehole in Jameson land, East Greenland – an introduction. In: Ineson, J. & Bojesen-Koefoed, J.A. (eds): Petroleum geology of the Upper Jurassic – Lower Cretaceous of East and North-East Greenland: Blokelv-1 borehole, Jameson Land Basin. Geological Survey of Denmark and Greenland Bulletin **42**, 7–14 (this volume).

Bjerager, M., Kjøller, C., Olivarius, M., Olsen, D. & Schovsbo, N. 2018a: Sedimentology, geochemistry and reservoir properties of Upper Jurassic deep marine sediments (Hareelv Formation) in the Blokelv-1 borehole, Jameson Land Basin, East Greenland. In: Ineson, J. & Bojesen-Koefoed, J.A. (eds): Petroleum geology of the Upper Jurassic – Lower Cretaceous of East and North-East Greenland: Blokelv-1 borehole, Jameson Land Basin. Geological Survey of Denmark and Greenland Bulletin **42**, 39–64 (this volume).

Bojesen-Koefoed, J.A., Peter Nytoft, H.P., Petersen, H.I., Piasecki, S. & Pilgaard, A. 2018: Petroleum potential of the Upper Jurassic Hareelv Formation, Jameson Land, East Greenland. In: Ineson, J. & Bojesen-Koefoed, J.A. (eds): Petroleum geology of the Upper Jurassic – Lower Cretaceous of East and North-East Greenland: Blokelv-1 borehole, Jameson Land Basin. Geological Survey of Denmark and Greenland Bulletin **42**, 85–113 (this volume).

Bonow, J.M., Japsen, P. & Nielsen, T.F.D. 2014: High-level landscapes along the margin of East Greenland – a record of tectonic uplift and incision after breakup in the NE Atlantic. Global and Planetary Change **116**, 10–29.

Brooks, C.K. 2011: The East Greenland rifted volcanic margin. Geological Survey of Denmark and Greenland Bulletin **24**, 96 pp.

Burnham, A.K. & Sweeney, J.J. 1989: A chemical kinetic model of vitrinite reflectance maturation. Geochimica et Cosmochimica Acta **53**, 2649–2657.

Christiansen, F.G., Larsen, H.C., Marcussen, C., Hansen, K., Krabbe, H., Larsen, L.M., Piasecki, S., Stemmerik, L. & Watt, J.W. 1992: Uplift study of the Jameson Land basin, East Greenland. Norsk Geologisk Tidsskrift **72**, 291–294.

Clausen, L. 1998: Late Neogene and Quaternary sedimentation on the continental slope and upper rise offshore Southeast Greenland: Interplay of contour and turbidity processes. In: Saunders, A.D *et al*. (eds): Proceedings of the Ocean Drilling Program, Scientific Results **152**, 3–18.

Green, P.F. & Duddy, I.R. 2012: Thermal history reconstruction in sedimentary basins using apatite fission-track analysis and related techniques. In: Harris, N.B. & Peters, K.E. (eds): Analyzing the thermal history of sedimentary basins: methods and case studies. SEPM Special Publication **103**, 65–104.

Green, P.F., Lidmar-Bergström, K., Japsen, P., Bonow, J.M. & Chalmers, J.A. 2013: Stratigraphic landscape analysis, thermochronology and the episodic development of elevated passive continental margins. Geological Survey of Denmark and Greenland Bulletin **30**, 150 pp.

Hald, N., Tegner, C. 2000: Composition and age of tertiary sills and dykes, Jameson Land Basin, East Greenland: relation to regional flood volcanism. Lithos **54**, 207–233.

Hansen, K., Bergman, S.C. & Henk, B. 2001: The Jameson Land basin (east Greenland): a fission track study of the tectonic and thermal evolution in the Cenozoic North Atlantic spreading regime. Tectonophysics **331**, 307–339.

Ineson, J. & Bojesen-Koefoed, J.A. (eds): Petroleum geology of the Upper Jurassic – Lower Cretaceous of East and North-East Greenland: Blokelv-1 borehole, Jameson Land Basin. Geological Survey of Denmark and Greenland Bulletin **42**, 168 pp. (this volume).

Japsen, P., Green, P.F., Bonow, J.M., Nielsen, T.F.D., & Chalmers, J.A. 2014: From volcanic plains to glaciated peaks: Burial and exhumation history of southern East Greenland after opening of the NE Atlantic. Global and Planetary Change **116**, 91–114.

Larsen, H.C. & Saunders, A.D. 1998: Tectonism and volcanism at

the southeast Greenland rifted margin: a record of plume impact and later continental rupture. In: Saunders, A.D. *et al*. (eds): Proceedings of the Ocean Drilling Program, Scientific Results **152**, 503–533.

Larsen, H.C., Saunders, A.D., Clift, P.D. *et al*. 1994: 13. Summary and principal results, Proceedings of the Ocean Drilling Program, Initial Reports **152**, 279–292.

Larsen L.M. 2018: Igneous intrusions in the cored Upper Jurassic succession of the Blokelv-1 core, Jameson Land Basin, East Greenland. In: Ineson, J & Bojesen-Koefoed, J.A. (eds): Petroleum geology of the Upper Jurassic – Lower Cretaceous of East and North-East Greenland: Blokelv-1 borehole, Jameson Land Basin. Geological Survey of Denmark and Greenland **42**, 127–132 (this volume).

Larsen, L.M., Pedersen, A.K., Sørensen, E.V., Watt, W.S. & Duncan, R.A. 2013: Stratigraphy and age of the Eocene Igtertivâ Formation basalts, alkaline pebbles and sediments of the Kap Dalton Group in the graben at Kap Dalton, East Greenland. Geological Society of Denmark Bulletin **61**, 1–18.

Larsen, L.M., Watt, W.S. & Watt, M. 1989: Geology and petrology of the Lower Tertiary plateau basalts of the Scoresby Sund region, East Greenland. Grønlands Geologiske Undersøgelse Bulletin **169**. 164 pp.

Larsen, M., Heilmann-Clausen, C., Piasecki, S. & Stemmerik, L. 2005: At the edge of a new ocean: post-volcanic evolution of the Palaeogene Kap Dalton Group, East Greenland. In: Doré, A.G. & Vining, B. (eds): Petroleum Geology: North-West Europe and Global Perspectives-Proceedings of the 6th Petroleum Geology Conference. Geological Society (London) 923–932.

Mathiesen, A., Bidstrup, T. & Christiansen, F.G. 2000: Denudation and uplift history of the Jameson Land basin, East Greenland – constrained from maturity and apatite fission data. Global and Planetary Change **24**, 275–301.

Neuhoff, P.S., Watt, W.S., Bird, D.K. & Pedersen, A.K. 1997: Timing and structural relations of regional zeolite zones in basalts of the East Greenland continental margin. Geology **25**, 803–806.

Newman, J. 1997: New approaches to detection and correction of suppressed vitrinite reflectance. Australian Petroleum Production & Exploration Association (APPEA) Journal **27**, 524–535.

Pedersen, A.K., Watt, M., Watt, W.S. & Larsen, L.M. 1997: Structure and stratigraphy of the Early Tertiary basalts of the Blosseville Kyst, East Greenland. Journal of the Geological Society (London) **154**, 565–570.

Price, S., Brodie, J., Whitham, A. & Kent, R. 1997: Mid-tertiary rifting and magmatism in the Traill O region, East Greenland. Journal of the Geological Society (London) **154**, 419–434.

Surlyk, F. 2003: The Jurassic of East Greenland: a sedimentary record of thermal subsidence, onset and culmination of rifting. In: Ineson, J. & Surlyk, F. (eds): The Jurassic of Denmark and Greenland. Geological Survey of Denmark and Greenland Bulletin **1**, 659–722.

Thomson, K., Green, P.F., Whitham, A.G., Price, S.P. & Underhill, J.R. 1999: New constraints on the thermal history of North-East Greenland from apatite fission-track analysis. Geological Society of America Bulletin **111**, 1054–1068.

Wilkins, R.W.T., Wilmshurt, J.R., Russel, N.J., Hladky, G., Ellacott, M.W. & Buckingham, C. 1992: Fluorescence alteration and the suppression of vitrinite reflectance. Organic Geochemistry **18**, 629–640.

Manuscript received 16 December 2015; revision accepted 8 February 2018

Appendix 1: Analytical details of the AFTA data

This appendix documents the raw fission-track count data together with radial/compositional graphical plots. The location of the two samples (GC1052-1, GC1052-2) in the Blokelv-1 core is indicated in Fig. 1.

Sample GC1052-1: Apatite

Slide ref	Current grain no	N_s	N_i	N_a	ρ_s	ρ_i	RATIO	U (ppm)	Cl (wt%)	FT Age (Ma)
G1124-9	3	1	23	36	4.414E+04	1.015E+06	0.043	8.1	0.04	12.2 ± 12.4
G1124-9	6	14	51	24	9.270E+05	3.377E+06	0.275	27.0	0.03	76.4 ± 23.1
G1124-9	7	0	13	49	0.000E+00	4.216E+05	0.000	3.4	0.14	0.0 ± 36.1
G1124-9	10	29	129	30	1.536E+06	6.833E+06	0.225	54.7	0.01	62.6 ± 13.0
G1124-9	11	18	48	24	1.192E+06	3.178E+06	0.375	25.4	0.06	104.1 ± 28.9
G1124-9	12	6	35	60	1.589E+05	9.270E+05	0.171	7.4	0.05	47.8 ± 21.2
G1124-9	13	27	96	60	7.151E+05	2.543E+06	0.281	20.3	0.02	78.2 ± 17.2
G1124-9	14	6	53	42	2.270E+05	2.005E+06	0.113	16.0	0.03	31.6 ± 13.6
G1124-9	15	54	339	20	4.290E+06	2.693E+07	0.159	215.6	0.11	44.4 ± 6.6
G1124-9	16	4	33	35	1.816E+05	1.498E+06	0.121	12.0	0.00	33.8 ± 17.9
G1124-9	17	1	13	60	2.648E+04	3.443E+05	0.077	2.8	0.08	21.5 ± 22.3
G1124-9	18	9	110	42	3.405E+05	4.162E+06	0.082	33.3	0.03	22.9 ± 8.0
G1124-9	19	5	18	30	2.648E+05	9.534E+05	0.278	7.6	0.02	77.3 ± 39.1
G1124-9	20	19	49	80	3.774E+05	9.733E+05	0.388	7.8	0.02	107.6 ± 29.2
G1124-9	21	4	32	70	9.080E+04	7.264E+05	0.125	5.8	0.02	34.9 ± 18.5
G1124-9	22	31	234	80	6.158E+05	4.648E+06	0.132	37.2	0.03	37.0 ± 7.1
G1124-9	23	11	113	50	3.496E+05	3.591E+06	0.097	28.7	0.03	27.2 ± 8.6
G1124-9	25	4	27	50	1.271E+05	8.581E+05	0.148	6.9	0.02	41.3 ± 22.2
G1124-9	28	1	6	100	1.589E+04	9.534E+04	0.167	0.8	0.07	46.5 ± 50.2
G1124-9	32	25	93	50	7.945E+05	2.956E+06	0.269	23.7	0.21	74.8 ± 17.0
		269	1515		4.309E+05	2.427E+06		19.4		

For abbreviations, see page 147
Area of basic unit = 6.293E+07 cm^2
χ^2 = 47.992 with 19 degrees of freedom
$P(\chi^2)$ = 0.0%

Age Dispersion = 38.770%
N_s / N_i = 0.178 ± 0.012
Mean Ratio = 0.176 ± 0.024
Pooled age = 49.5 ± 3.6 Ma
Central age = 50.4 ± 6.2 Ma

Age calculated using a zeta of 392.9 ± 7.4 for CN5 glass
ρ_D = 1.424E+06 cm^2 ND = 2241
ρ_D interpolated between top of can; ρ_D = 1.388E+06 cm^2 ND = 1092
ρ_D interpolated between bottom of can; ρ_D = 1.461E+06 cm^2 ND = 1149

Radial plot of single grain ages*

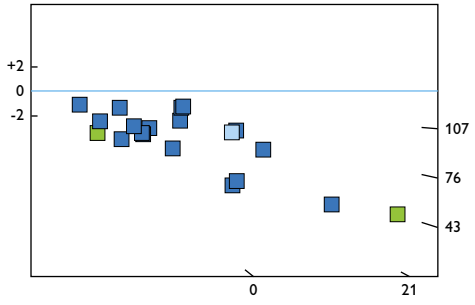

* See Appendix B in Geotrack Report GC1052 (available online) for details of radial plot construction. Colour datapoints indicate wt% Cl: Dark blue: <0.1%. Green: 0.1-0.2%. Pale blue: 0.2-0.3%.

Distribution of Chlorine (Cl) contents in apatite grains

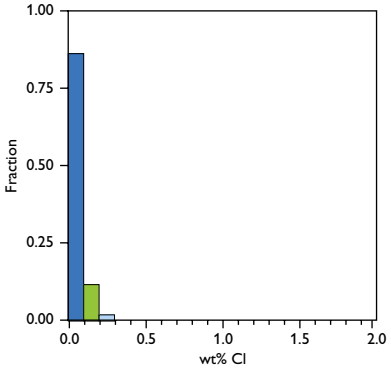

Single grain age vs. weight % Cl for individual apatite grains

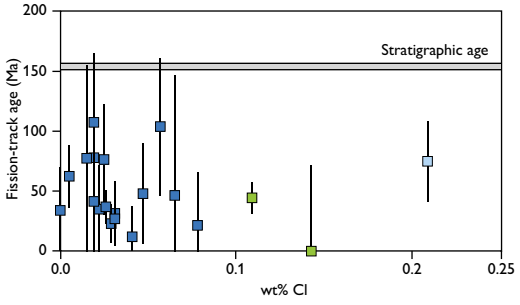

Distribution of confined track lengths

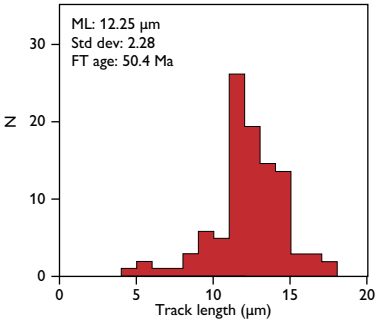

Sample GC1052-2: Apatite

Slide ref	Current grain no	N_s	N_i	N_a	ρ_s	ρ_i	RATIO	U (ppm)	Cl (wt%)	FT Age (Ma)
G1124-10	3	15	84	50	4.767E+05	2.670E+06	0.179	21.3	0.23	49.9 ± 14.1
G1124-10	4	5	31	70	1.135E+05	7.037E+05	0.161	5.6	0.20	45.1 ± 21.8
G1124-10	10	7	56	50	2.225E+05	1.780E+06	0.125	14.2	0.01	35.0 ± 14.1
G1124-10	11	9	126	30	4.767E+05	6.674E+06	0.071	53.2	0.01	20.0 ± 6.9
G1124-10	12	3	63	28	1.703E+05	3.575E+06	0.048	28.5	0.02	13.4 ± 7.9
G1124-10	14	41	198	35	1.861E+06	8.990E+06	0.207	71.7	0.08	57.9 ± 10.1
G1124-10	15	14	94	36	6.180E+05	4.149E+06	0.149	33.1	0.01	41.7 ± 12.0
G1124-10	16	1	12	28	5.675E+04	6.810E+05	0.083	5.4	0.02	23.4 ± 24.3
G1124-10	17	9	48	48	2.980E+05	1.589E+06	0.188	12.7	0.10	52.4 ± 19.1
G1124-10	19	5	54	30	2.648E+05	2.860E+06	0.093	22.8	0.03	25.9 ± 12.1
G1124-10	21	16	152	40	6.356E+05	6.038E+06	0.105	48.2	0.04	29.5 ± 7.8
G1124-10	22	7	35	40	2.781E+05	1.390E+06	0.200	11.1	0.02	55.9 ± 23.2
G1124-10	23	5	54	40	1.986E+05	2.145E+06	0.093	17.1	0.14	25.9 ± 12.1
G1124-10	24	15	86	35	6.810E+05	3.905E+06	0.174	31.1	0.00	48.8 ± 13.7
G1124-10	25	10	57	42	3.783E+05	2.157E+06	0.175	17.2	0.00	49.1 ± 16.9
G1124-10	26	8	93	36	3.531E+05	4.105E+06	0.086	32.7	0.02	24.1 ± 8.9
G1124-10	29	7	101	70	1.589E+05	2.293E+06	0.069	18.3	0.00	19.4 ± 7.6
G1124-10	30	21	84	40	8.343E+05	3.337E+06	0.250	26.6	0.01	69.8 ± 17.1
G1124-10	33	0	7	40	0.000E+00	2.781E+05	0.000	2.2	0.02	0.0 ± 74.1
G1124-10	34	17	95	40	6.754E+05	3.774E+06	0.179	30.1	0.04	50.0 ± 13.3
		215	1530		4.126E+05	2.936E+06		23.4		

For abbreviations, see page 147
Area of basic unit = 6.293E-07 cm^2
χ^2 = 32.061 with 19 degrees of freedom
$P(\chi^2)$ = 3.1%

Age Dispersion = 27.489%
N_s / N_i = 0.141 ± 0.010
Mean Ratio = 0.132 ± 0.014
Pooled age = 39.3 ± 3.1 Ma
Central age = 38.5 ± 4.0 M

Age calculated using a zeta of 392.9 ± 7.4 for CN5 glass
ρ_D = 1.429E+06 cm^2 ND = 2241
ρ_D interpolated between top of can; ρ_D = 1.388E+06 cm^2 ND = 1092
ρ_D interpolated between bottom of can; ρ_D = 1.461E+06 cm^2 ND = 1149

Radial plot of single grain ages*

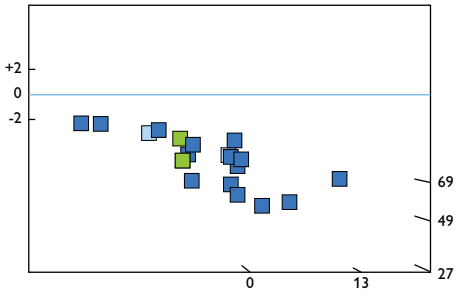

* See Appendix B in Geotrack Report GC1052 (available online) for details of radial plot construction. Colour datapoints indicate wt% Cl: Dark blue: <0.1%. Green: 0.1-0.2%. Pale blue: 0.2-0.3%. Purple: >0.3%.

Distribution of Chlorine (Cl) contents in apatite grains

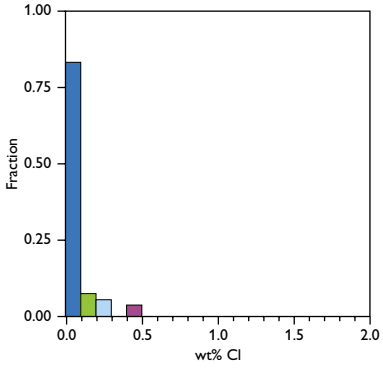

Single grain age vs. weight % Cl for individual apatite grains

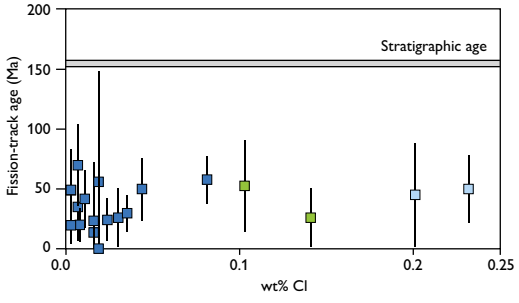

Distribution of confined track lengths

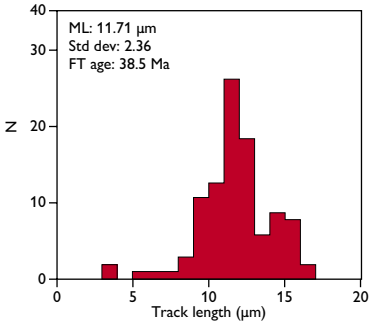

Table abbreviations

N_a	=	Number of grid squares counted in each grain
N_s	=	Number of spontaneous tracks in N_a grid squares
N_i	=	Number of induced tracks in N_a grid squares
RATIO	=	N_s/N_i
U (ppm)	=	Uranium content of each grain (= U content of standard glass × ρ_i/ρ_D)
Cl (wt%)	=	Weight percent chlorine content of each grain
ρ_s	=	Spontaneous track density (ρ_s) = N_s/ (N_a × area of basic unit)
ρ_i	=	Induced track density (ρ_i) = N_i/(N_a × area of basic unit)
FT age	=	Fission-track age, calculated using equation B.1
Area of basic unit	=	Area of one grid square
Chi squared	=	χ^2 parameter, used to assess variation of single grain ages within the sample
P(chi squared)	=	Probability of obtaining observed χ_2 value for the relevant number of degrees of freedom, if all grains belong to a single population
Age Dispersion	=	% variation in single grain ages
N_s/N_i	=	Pooled ratio, total spontaneous tracks divided by total induced tracks for all grains
Mean ratio	=	Mean of (N_s/N_i) for individual grains
Zeta	=	Calibration constant, determined empirically for each observer
ρ_D	=	Track density (ρ_D) from uranium standard glass (interpolated from values at each end of stack)
N_D	=	Total number of tracks counted for determining ρ_D
Pooled age	=	Fission track age calculated from pooled ratio N_s/N_i. Valid only when $P(\chi^2)$ >5%
Central age	=	Alternative to pooled age when $P(\chi^2)$ <5%